

# Filtrated Common Functional Principal Components of Multi-group Functional data

Shuhao Jiao<sup>\*1</sup>, Ron D. Frostig<sup>†2</sup>, and Hernando Ombao<sup>‡1</sup>

<sup>1</sup>Statistics Program, KAUST, Saudi Arabia

<sup>2</sup>Department of Neurobiology and Behavior, UC Irvine, USA

## Abstract

Local field potentials (LFPs) are signals that measure electrical activity in localized cortical regions from implanted tetrodes in the human or animal brain. The LFP signals are curves observed at multiple tetrodes which are implanted across a patch on the surface of the cortex. Hence, they can be treated as multi-group functional data, where the trajectories collected across temporal epochs from one tetrode are viewed as a group of functions. In many cases, multi-tetrode LFP trajectories contain both global variation patterns (which are shared in common to all groups, due to signal synchrony) and isolated variation patterns (common only to a small subset of groups), and such structure is very informative to the analysis of such data. Therefore, one goal in this paper is to develop an efficient procedure that is able to capture and quantify both global and isolated features. We propose a novel tree-structured functional principal components (filt-fPC) analysis through finite-dimensional functional representation – specifically via filtration. A major advantage of the proposed filt-fPC method is the ability to extract the components that are common to multiple groups (or tetrodes) in a flexible "multi-resolution" manner and simultaneously preserve the idiosyncratic individual components of different tetrodes. The proposed filt-fPC approach is highly data-driven and no "ground-truth" model pre-specification is needed, making it a suitable approach for analyzing multi-group functional data that is complex. In addition, the filt-fPC method is able to produce a parsimonious, interpretable, and efficient low dimensional representation of multi-group functional data with orthonormal basis functions. Here, the proposed filt-fPCA method is employed to study the impact of a shock (induced stroke) on the synchrony structure of the rat brain. The proposed filt-fPCA is a general approach that can be readily applied to analyze other complex multi-group functional data, such as multivariate functional data, spatial-temporal data and longitudinal functional data.

---

<sup>\*</sup>shjiaoqd@gmail.com

<sup>†</sup>rfrostig@uci.edu

<sup>‡</sup>hernando.ombao@kaust.edu.sa

**Key words:** Functional principal components, Community detection, Dimension reduction, Multi-group functional data, Network filtration, Unsupervised learning, Weighted network.

# 1 Introduction

## 1.1 Data description and statistical challenges

This work is motivated by a neuroscience study conducted by co-author, Ron D. Frostig, where the goal is to investigate the impact of an extreme shock (such as a stroke) on the functional organization of the rat brain. In the experiment described in Wann (2017), ischemic stroke was simulated by clamping the medial cerebral artery of a rat. Brain activity was continuously monitored over several hours (both pre-occlusion and post-occlusion/clamping) through the local field potential (LFP) recordings from 32 implanted micro-tetodes (the placement of the 32 micro-tetodes is shown in the supplementary material). In this set-up, two temporal phases of the LFP recordings were considered: pre-occlusion and post-occlusion.

The LFP plots for one pre-occlusion epoch from the first 15 tetodes are shown in Figure 1. The plots convey that some tetodes produce trajectories displaying similar variation patterns due to signal synchrony, and the level of synchrony is not the same across tetodes. It is potentially critical to check how synchrony is affected by ischemic stroke for understanding how the temporal coordination in the function of large-scale brain networks are associated with the functional impairments caused by ischemia.

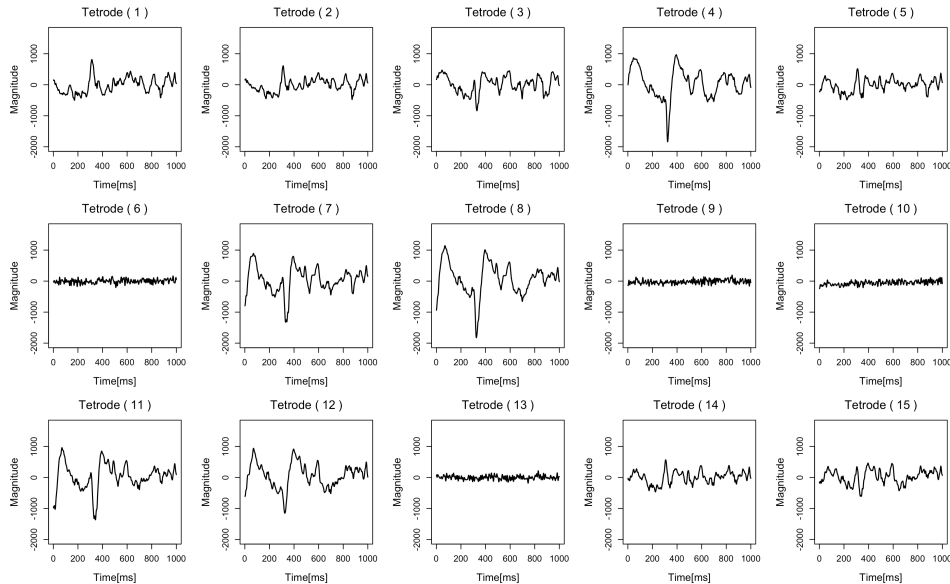


Figure 1: One pre-occlusion epoch (1 second) of the first 15 tetodes

Since the mean curves are always close to zero for brain signals, one goal in dimension

reduction of such functional data is to identify the commonality of covariance structures across different tetrodes, which is highly associated with synchrony in this neuroscience project. Here, we say "covariance structure" instead of "covariance operator" because the major interest is the variation pattern rather than the variation level. As the covariance structure of different tetrodes can be quite similar due to the synchrony phenomenon, it is possible to obtain a more parsimonious representation – via the filt-fPCA – by employing common components across different tetrodes. Such common components are informative to the synchrony structure of multi-tetrode LFPs.

Note that signal synchrony is just a special reason that leads to the feasibility of employing common principal components. Two groups of functions can share common principal components as long as they share similar covariance structure. In this paper, the developed new method has the ability to extract the common components for general multi-group functional data. In this paper, the focus will be on the 10-minute period around the time of occlusion: 5 minutes immediately prior to occlusion of the medial cerebral artery (pre-occlusion) and 5 minutes during the post-occlusion phase. The goal is not to classify the signals into pre-occlusion vs post-occlusion phases. Rather, the aims are (i.) to extract the *intrinsic* functional structure that is present during each phase respectively; and (ii.) to identify and quantify the differences in the functional structure between the two phases. To conduct our analysis, the LFP data was segmented into separate 1-second epochs and thus, each of the pre-occlusion and post-occlusion phases consists of 300 epochs for each tetrode.

## 1.2 Existing fPCA methods for multivariate functional data

Functional data analysis is an active area primarily driven by its wide range of potential applications. Due to the infinite dimensionality of functional data, one of the fundamental techniques employed in the analysis is dimension reduction. Functional principal component analysis (fPCA), as described in Ramsay & Silverman (2004), is a widely-applied dimension reduction technique for univariate functional data analysis because it gives the optimal approximation of functions (with respect to the integrated squared error of reconstruction) and at the same time yields results that are interpretable in the sense that it captures the principal directions of variation. More work on fPCA include, but are not limited to, Hall & Hosseini-Nasab (2006), Hall et al. (2006), Yao & Lee (2006), Yao (2007), Jiang & Wang (2010), Bali et al. (2011).

In many experiments, multiple groups of functional trajectories are collected for a sample of experimental units. There is a need for statistical methods to account for the common variation patterns of multiple groups of functions, which, in our application, are present across tetrodes in both the pre-occlusion and post-occlusion phases. However, there are only a few methods that are appropriate for this type of functional data. We now describe these methods and discuss the advantages of filt-fPCA.

The naive approach of applying ordinary univariate fPCA by lumping all groups into one big group may not be suitable for multi-group functional data, especially when there

is substantial variation in the covariance functions of different groups. Consequently, the fPCs obtained are not guaranteed to be capable of explaining the major variation in *all* groups. At the other end of this spectrum, employing group-wise fPCs to each group separately can be problematic as well, because this leads to a large number of distinct fPCs when the number of groups is large and cannot reveal the connection between different groups. Several methods of functional principal component analysis for multivariate functional data have been recently developed. A multilevel functional principal components method is proposed in Di et al. (2009) which explains the variation both within and between different groups of functions. This was extended to sparse sampled multilevel functional data in Di et al. (2014). In Kayano & Konishi (2009), functional principal component analysis has been developed for multivariate functions with Gaussian-shape basis. Berrendero et al. (2011) proposed the multivariate principal component with functional scores. A framework for longitudinal functional principal components in Greven et al. (2011) combines the covariance of within-subject and between-subject components. A two-step fPCA method for longitudinal functional data has been developed in Chen & Müller (2012) where the fPCA is implemented according to different longitudinal indexes, and the resulting principal components vary as the longitudinal index changes. An extension is proposed in Chen et al. (2017) which gives a framework with a more parsimonious fPC representation – marginal fPC representation Chiou et al. (2014) and Jacques & Preda (2014) proposed the multivariate functional principal component analysis (MfPCA) which describe the variation pattern of multivariate functional data, and Happ & Greven (2018) extended the MfPCA for functions defined over different domains. In contrast to the existing methods, one major advantage of filt-fPCA is that it has the ability to produce flexible and efficient (in functional reconstruction) fPC commonality structures, giving a "multi-layer analysis" which identifies the global structure (common across groups) and local structure (group-specific), and works for both balanced and unbalanced design.

There are also methods on principal component analysis of multi-group multivariate data. Common principal component analysis (CPCA, see e.g., Flury (1984), Benko et al. (2009)) and partial common principal component analysis (PCPCA, see e.g., Flury (1987), Schott (1999), Wang et al. (2019)) are two classes of methods developed for finding the common principal component for multi-group multivariate data. In Crainiceanu et al. (2011), a population value decomposition (PVD) procedure is proposed. Moreover, Lock et al. (2013) and Feng et al. (2018) proposed JIVE and AJIVE procedures to extract common and individual components for multi-block data. While some of the existing methods (i.e., CPCA and PCPCA) and the proposed filt-fPCA share the same goal of finding a common "representation" of multi-group functional data, the principles and algorithms are different. In CPCA and PCPCA, all groups are assumed to share the same set of common principal components, and the focus is on testing the "commonality". Such assumption can be overly restrictive practically. Comparatively, the filt-fPCA aims to find a reasonable common fPC system, and has the ability of extracting "multi-resolution" common features of different groups. More details will be discussed.

### 1.3 Filtrated functional principal component analysis

In this article, we propose a new procedure to extract common fPCs (filt-fPCs) that produces a low-dimensional representation for multi-group functional data. The filt-fPCA method builds on the idea of filtration in network analysis and extracts the common principal components via multi-layer filtrations.

The *fundamental philosophy* of filt-fPCA is that, as the common components are extracted from the different tetrodes/groups of functions (here, epoch curves) with an increasing number of layers, the components of residuals across different groups tend to be more idiosyncratic. Therefore, we propose to employ a tree-structured common fPC system as displayed in Figure 2. Define a *community* as a collection of multiple tetrodes/groups of functions. As the filtration goes, all groups are layer-wisely split into smaller communities, where "higher-resolution" (more group-specific) common components are to be extracted. The communities in a layer are always nested in, or identical to, the communities of the previous layer. The filt-fPCs in the first layer of the tree structure capture the most common variation pattern, and the filt-fPCs in the layers formed later in the tree pertain to more idiosyncratic variation patterns which are shared by a fewer number of tetrodes/groups. For each community, one common filt-fPC is extracted for all tetrodes/groups of functions belonging to that community. Clearly, a primary step before obtaining filt-fPCs is to find a decent *community structure* which includes the communities in all incorporated layers.

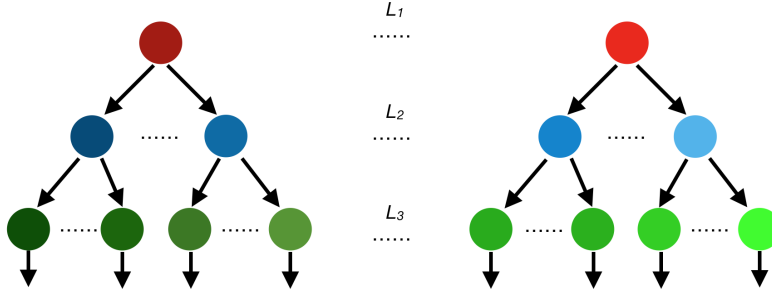


Figure 2: Hierarchical tree structure of filt-fPCs. Here,  $L_j$  signifies the  $j$ -th layer of filtration. Different communities are represented by different colored solid circles. Note that there can be multiple trees since the groups may be partitioned into multiple communities in the first layer (one tree per first-layer community).

In summary, the proposed filt-fPCA method has the following advantages: 1.) The method is data-driven without constraints of model specification, and no prior knowledge is needed to implement the method, making it suitable for complex multi-group functional data. 2.) The method produces functional principal components that simultaneously reveal both the common and individual features of various groups of functions in a "multi-resolution" manner, which enables sophisticated analysis and provides more comprehensive explanation of multi-group functional data. (see Section 5) 3.) The method produces basis functions that are orthonormal for each group and thus greatly reduces computational burden in the sequential analysis. (see Section 3.3) 4.) The

proposed method is applicable to both balanced and unbalanced design of multi-group functional data.

The rest of the paper is organized as follows. In Section 2, some preliminaries of functional data are introduced. In Section 3, we develop the filt-fPCA procedure, including network filtration, community detection and selection, and computing of filtrated functional principal component. Section 4 presents some simulation results. Section 5 presents the real data analysis on the local field potentials of rat brain activity. Conclusions and summaries are made in Section 6. Technical proofs, pseudocode, and additional figures can be found in the supplementary material.

## 2 Preliminaries

Denote  $X(t) \in L_H^p = L_H^p(\Omega, \mathcal{A}, \mathbb{P})$  to be such that, for some  $p > 0$ , a  $H$ -valued function  $X(t)$  satisfies  $E\{\|X(t)\|^p\} < \infty$ . Here  $\|\cdot\|$  is the  $\ell^2$ -norm defined for elements in  $H$ . In what follows, all trajectories  $\{X_n(t): n \in \mathbb{N}\}$  are assumed to be functions defined in the Hilbert space  $L^2[0, 1]$ , where the inner product is defined as  $\langle x, y \rangle = \int_0^1 x(t)y(t)dt$ , and the norm is defined as  $\|x\|^2 = \int_0^1 x(t)^2 dt < \infty$ . Suppose that  $X(t) \in L_H^1$ , then the mean function is defined to be  $\mu(t) = E\{X(t)\}$ . Moreover, if  $X(t) \in L_H^2$ , then the covariance operator is defined to be  $\Gamma: L^2[0, 1] \rightarrow L^2[0, 1]$  by  $\Gamma(\cdot) = E\{\langle X - \mu, \cdot \rangle (X - \mu)(t)\}$ .

By the Mercer's theorem, the following expression holds for the covariance operator  $\Gamma(\cdot)$ ,  $\Gamma(\cdot) = \sum_{j=1}^{\infty} \theta_j \langle \nu_j, \cdot \rangle \nu_j(t)$ , where  $\{\theta_j: j \in \mathbb{N}_+\}$  are the positive eigenvalues (in strictly descending order) and  $\{\nu_j(t): j \in \mathbb{N}_+\}$  are the corresponding normalized eigenfunctions, so that  $\Gamma(\nu_j) = \theta_j \nu_j$  and  $\|\nu_j\| = 1$ . Here,  $\{\nu_j(t): j \in \mathbb{N}_+\}$  forms a sequence of orthonormal bases for  $L^2[0, 1]$ . Let  $\{X_n(t): n \in \mathbb{N}\}$  be a sequence of random functions with mean function  $\mu(t)$  and covariance operator  $\Gamma(\cdot)$ . By the Karhunen-Loève theorem, under mild conditions,  $X_n(t)$  admits the representation  $X_n(t) = \mu(t) + \sum_{j=1}^{\infty} \langle X_n - \mu, \nu_j \rangle \nu_j(t)$ . Suppose that there are  $N$  samples  $X_1(t), \dots, X_N(t)$ , then the estimator of  $\mu(t)$  is  $\hat{\mu}(t) = N^{-1} \sum_{n=1}^N X_n(t)$ , and the estimator of the covariance operator is given by  $\hat{\Gamma}(\cdot) = N^{-1} \sum_{n=1}^N \langle X_n - \hat{\mu}, \cdot \rangle (X_n - \hat{\mu})(t)$ .

Suppose that there are  $G$  groups of functions  $\{X_{vn}(t): v = 1, \dots, G, n \in \mathbb{N}\}$ , where  $X_{vn}(t)$  is the  $n$ -th function in group  $v$ . Without loss of generality, assume the mean function of each group  $v$  is zero. Then for a community  $\mathcal{K}$  including some of the groups, the leading common filtrated functional principal component is defined as  $\arg \min_{\|\phi\|=1} \sum_{v \in \mathcal{K}} f_v E\|X_{vn} - \langle X_{vn}, \phi \rangle X_{vn}\|^2$ , where  $\{f_v: v = 1, \dots, G\}$  specifies the weight of different groups. A large value of  $f_v$  leads to higher influence of the corresponding group on the common filt-fPC.

**Remark 1.**  $\{f_v: v = 1, \dots, G\}$  should be specified according to specific needs. As a special case, if all groups are equally important, one appropriate way to specify  $\{f_v: v = 1, \dots, G\}$  is  $f_v = 1 / \sum_{j \geq 1} \theta_{vj}$ , where  $\theta_{vj}$  is the  $j$ -th eigenvalue of the covariance operator of the  $v$ -th group.

The following proposition provides some guidance to find the leading filt-fPC for a given community  $\mathcal{K}$ .

**Proposition 1.** Suppose that, for each  $v \in \mathcal{K}$ ,  $X_{vn}(t) \in L_H^2$ . The minimizer of  $\sum_{v \in \mathcal{K}} f_v E \|X_{vn} - \langle X_{vn}, \phi \rangle \phi\|^2$  under  $\|\phi\| = 1$  is the eigenfunction corresponding to the largest eigenvalue of  $\sum_{v \in \mathcal{K}} f_v \Gamma_v(\cdot)$ , where  $\Gamma_v(\cdot) = E\{\langle X_{vn}, \cdot \rangle X_{vn}\}$ .

**Remark 2.** Proposition 1 provides a blueprint for obtaining the filt-fPCs given a community. In practice, we replace  $\sum_{v \in \mathcal{K}} f_v \Gamma_v(\cdot)$  with its empirical version  $\sum_{v \in \mathcal{K}} f_v \hat{\Gamma}_v(\cdot)$ .

## 3 Network model and filtrated fPCA

### 3.1 The filt-fPC representation

Recall that our primary aim is to find the principal components that jointly explain the variation of multiple groups in a filtrating manner, i.e., to obtain the common filt-fPCs for each of the tree-structured communities, and a community is defined to be a set of groups where one common filt-fPC is employed for all the groups in that set. The first layer filt-fPCs capture the most common variation pattern, and over the sequence of the filtrations, the filt-fPCs tend to reveal more localized (shared by smaller communities) and idiosyncratic individual variation features. The key idea of filt-fPCA is to represent  $\{X_{vn}(t) : v = 1, \dots, G, n = 1, \dots, N_v\}$  in the following form,

$$X_{vn}(t) = \mu_v(t) + \sum_{d=1}^{\infty} \langle X_{vn} - \mu_v, \phi_d^{(c_{v,d})} \rangle \phi_d^{(c_{v,d})}(t), \quad (3-1)$$

where  $c_{v,d}$  is the community index of group  $v$  in the  $d$ -th layer of filtration,  $\{\phi_d^{(c_{v,d})}(t) : d \geq 1\}$  are the filt-fPCs of group  $v$  (group  $v$  and group  $v'$  share the same filt-fPC in dimension  $d$  if  $c_{v,d} = c_{v',d}$ ), and  $\mu_v(t)$  is the mean function of the  $v$ -th group, which is zero in our project since LFPs always oscillate around the zero-line.

We develop a novel data-adaptive method to find the community structure which will be discussed later. It can be shown that the resulting  $\{\phi_d^{(c_{v,d})} : d \geq 1\}$  is a series of orthonormal basis functions for group  $v$ , and hence adaptive to the unique feature of each layer  $d$ .  $\{\langle X_{vn} - \mu_v, \phi_d^{(c_{v,d})} \rangle : d \geq 1\}$  are the filt-fPC scores of  $X_{vn}(t)$ .

**Remark 3.** It is worth noting that, unlike CPCA and PCPCA, the numbers of shared common components are not required to be the same across groups in filt-fPCA.

**Remark 4.** Note that, since functional data is infinite-dimensional, a community structure can include up to infinitely many layers, and there exists at least one layer of structure shared across infinitely many consecutive layers, but in practice only a finite number of layers are incorporated since it is very hard to implement statistical analysis in an infinite-dimensional space. More details will be discussed in Section 3.4.

### 3.2 Weighted network, filtration, and community detection

A preliminary step is to evaluate the similarity of the covariance structures. To motivate our approach, we first develop the notion of similarity through a weighted network model. A weighted network is a triple  $(N, E, \omega)$ , where  $N$  is the node set representing groups,  $E$  is the edge set, and  $\omega$  is the set of edge weights. In our application, the nodes represent tetrodes; edges can be viewed as existence of synchrony between different regions of brain, which is complete (all pairs of nodes are connected) at the beginning of filtration since we have no prior knowledge that some pairs of regions are not synchronized at all; weights represent the similarity of covariance structures, and also reveal the level of synchrony. A *small* value of edge weight indicates *similar* variation pattern of the adjacent nodes (higher level of synchrony of the corresponding two tetrodes).

The principle is that, if two nodes are connected by an edge, then the functions in these two groups are considered to share some similar variation patterns, and thus likely share some common filt-fPCs. The edge weight  $\omega$  should be a reasonable measure of similarity between different covariance structures. Notationally, denote the weight of edge adjacent to nodes  $i$  and  $j$  as  $\omega_{ij}$ , and we propose to set  $\omega_{ij} = \|\mathcal{C}_i - \mathcal{C}_j\|_{\mathcal{S}}$ , where  $\mathcal{C}_i$  is the scaled covariance operator of the  $i$ -th group, defined as  $\mathcal{C}_i = \Gamma_i / \sum_{j \geq 1} \theta_{ij}$ ,  $\theta_{ij}$  is the  $j$ -th eigenvalue of  $\Gamma_i$ , and  $\|\cdot\|_{\mathcal{S}}$  denotes the Hilbert-Schmidt norm. The scaling step prevents the groups with high variation level from overly laying influence on the common filt-fPCs.

Network filtration is a multi-thresholding framework for displaying the dynamic pattern of how network features change over different thresholds. Here, we propose to specify a sequence of positive thresholds  $\{\tau_d: d \geq 1\}$  in non-ascending order ( $\tau_1 \geq \tau_2 \geq \tau_3 \geq \dots$ ). For each  $d$ , we eliminate the edges of which the weights are greater than the threshold  $\tau_d$ . Corresponding to the thresholds, a sequence of nested network are obtained after the edge truncation  $\{(N, E_d, \omega): d \geq 1\}$ , where  $E_1 \supseteq E_2 \supseteq \dots$ . Next apply our proposed community detection algorithm (see Section 3.5) to separate the nodes into different disjoint communities for each  $(N, E_d, \omega)$ . We illustrate the idea of filtration and community in Figure 3, where, in the first and second filtration layer, the nodes are separated into one and three communities, and thus one and three distinct filt-fPCs are obtained in the first two layers. The last filtration eliminates all the edges, so that all nodes are not connected and the filt-fPCs, starting from the third layer, pertain to the idiosyncratic variation pattern of each individual group. Details on our data-adaptive procedure of community selection will be discussed in Section 3.4.

### 3.3 Filtrated functional principal component

In this section, we demonstrate how to obtain the empirical filtrated functional principal components for each community. Denote  $\mathcal{K}_{d1}, \mathcal{K}_{d2}, \dots$  as the communities in the  $d$ -th layer and  $f_v^{(d)}$  as the positive weight of group  $v$  in the  $d$ -th layer, then the common



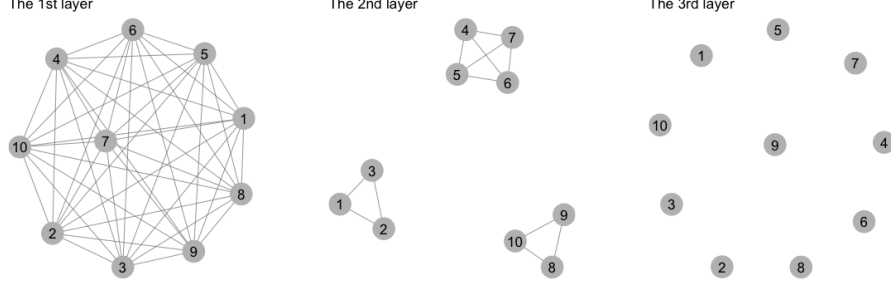


Figure 3: Network filtration and the community structure of the first three layers. Starting from the third layer, all nodes are separated from each other, and thus the following filt-fPCs pertain to only the individual variation patterns.

empirical filt-fPC of  $\mathcal{K}_{di}$ , denoted by  $\phi_{di}$ , is defined as:

$$\hat{\phi}_{di} = \arg \max_{\|\phi\|=1} \sum_{v \in \mathcal{K}_{di}} \sum_{n=1}^{N_v} \frac{f_v^{(d)}}{N_v} \langle R_{vn}^{(d-1)}, \phi \rangle^2, \quad \text{for } v \in \mathcal{K}_{di}, i \geq 1.$$

As illustrated in Proposition 1, the maximizer of the objective function

$$\sum_{v \in \mathcal{K}_{di}} \sum_{n=1}^{N_v} N_v^{-1} f_v^{(d)} \langle R_{vn}^{(d-1)}, \phi \rangle^2$$

is the first eigenfunction of the operator  $\sum_{v \in \mathcal{K}_{di}} f_v^{(d)} \hat{\Gamma}_v^{(d)}(\cdot)$ , where

$$\hat{\Gamma}_v^{(d)}(\cdot) = N_v^{-1} \sum_{n=1}^{N_v} \{R_{vn}^{(d-1)} \langle R_{vn}^{(d-1)}, \cdot \rangle\},$$

and  $R_{vn}^{(d)}(t) = X_{vn} - \sum_{j=1}^d \langle X_{vn}, \hat{\phi}_j^{(c_{v,j})} \rangle \hat{\phi}_j^{(c_{v,j})}$  and  $R_{vn}^{(0)}(t) = X_{vn}(t)$ .

**Remark 5.** If all groups are equally important in all layers, a proper way to specify  $f_v^{(d)}$  is  $f_v^{(d)} = 1 / \sum_{j \geq 1} \theta_{vj}^{(d-1)}$ , where  $\theta_{vj}^{(d-1)}$  is the  $j$ -th eigenvalue of the covariance operator of  $R_{vn}^{(d-1)}$ .

**Proposition 2.** The filtrated principal components  $\{\phi_d^{(c_{v,d})}(t) : d \geq 1\}$  are orthonormal for any  $v \geq 1$ .

**Remark 6.** This proposition is important in the sequential analysis, e.g., in the finite-dimensional projection of functional linear models, orthonormality avoids cross terms and hence leads to a concise finite-dimensional representation.

## 3.4 Selection of community structure

### 3.4.1 Generalized information criterion

Motivated by the generalized information criterion (GIC, see e.g., Nishii (1984) and Zhang et al. (2010)), we propose a penalized criterion, which follows the format: mea-

sure of model fit + tuning parameter  $\times$  measure of model complexity. The idea of adding this penalty comes from the fact that, if the groups are split into too many communities, the resulting filt-fPCs will very likely fail to capture the commonality of covariance structures well, although they are efficient in functional reconstruction.

For a given community structure  $\mathbf{C}_\alpha$  ( $\alpha$  is the index of community structure) and the corresponding empirical filt-fPCs  $\{\hat{\phi}_{\alpha,d}^{(c_{v,d})}(t), d \geq 1, v = 1, \dots, G\}$ , we define the GIC value to be

$$\text{GIC}(\mathbf{C}_{\alpha,1:D}) = - \sum_{v=1}^G N_v^{-1} f_v \left\{ \sum_{n=1}^{N_v} \sum_{d=1}^D \langle X_{vn}, \hat{\phi}_{\alpha,d}^{(c_{v,d})} \rangle^2 \right\} + \lambda_N(\aleph \mathbf{C}_{\alpha,1:D}), \quad (3-2)$$

where  $\aleph$  signifies the cardinality (the total number of communities), and  $\mathbf{C}_{\alpha,1:D}$  represents the first  $D$  layers of community structure  $\mathbf{C}_\alpha$ . Given  $D$ , the optimal community structure is defined as the minimizer of  $\text{GIC}(\mathbf{C}_{\alpha,1:D})$ .

To illustrate the large-sample property of the selected community structure, we now introduce the following concept. Let  $\{\phi_{vd}: d \geq 1\}$  be the ordinary group-wise fPCs of the  $v$ -th group, and the following concept quantifies the difference between the filt-fPCs and ordinary group-wise fPCs.

**Definition 1** ( $\tau$ -oracle community structure). A community structure  $\tilde{\mathbf{C}}_\tau$  is called the  $\tau$ -oracle community structure if, as  $D \rightarrow \infty$ ,  $\tilde{\mathbf{C}}_{\tau,1:D}$  asymptotically almost surely has the minimal cardinality among all the community structures satisfying the condition

$$\sigma_{\alpha,D} := E \left\{ \sum_{v=1}^G \sum_{d=1}^D \left( \langle X_{vn}, \phi_{vd} \rangle^2 - \langle X_{vn}, \hat{\phi}_{\alpha,d}^{(c_{v,d})} \rangle^2 \right) \right\} = O(D^{-\tau}).$$

**Remark 7.** Note that the "oracle" defined here is quite different from the traditional definition of "oracle", as we do not assume any "ground truth" model here. The developed method is data-driven, and is not constrained with any model pre-specification. The  $\tau$ -oracle community structure may not be identifiable, however, this should not be viewed as a problem, because the main goal here is to find a reasonable community structure but not to find a pre-specified community structure.

Given a value of  $\tau$  specified by the oracle, community structures are classified into three categories  $\mathcal{H}_{\tau,-}$  (under-fitted),  $\mathcal{H}_\tau$  and  $\mathcal{H}_{\tau,+}$  (over-fitted), defined respectively as

$$\begin{aligned} \mathcal{H}_{\tau,-} &= \{ \mathbf{C}_\alpha: \sigma_{\alpha,D} = O(D^{-\beta_{1,\alpha}}), \beta_{1,\alpha} < \tau \}, \\ \mathcal{H}_\tau &= \{ \mathbf{C}_\alpha: \sigma_{\alpha,D} = O(D^{-\tau}) \}, \\ \mathcal{H}_{\tau,+} &= \{ \mathbf{C}_\alpha: \sigma_{\alpha,D} = O(D^{-\beta_{2,\alpha}}), \beta_{2,\alpha} > \tau \}, \end{aligned}$$

and we make the following regularity assumptions. In the following, "const." signifies a positive constant.

**Assumption 1** ( $L^{4+\delta} - m$ -approximable, Hörmann & Kokoszka (2010)). There are  $G$  measurable functions  $f_1, \dots, f_G: S^\infty \rightarrow L^2(\mathcal{T})$ , where  $S$  is a measurable space, and

i.i.d. innovations  $\{\epsilon_i: i \in \mathbb{N}\}$  taking values in  $S$ , so that  $X_{vn}(t) = f_v(\epsilon_n, \epsilon_{n-1}, \dots)$ . It is assumed that  $E\|X_{vn}(t)\|^{4+\delta} < \infty$  for some  $\delta > 0$  and  $v = 1, \dots, G$ . In addition, for each  $v$ , there exists a  $m$ -dependent sequence  $\{X_{nv,m}(t): n \in \mathbb{N}\}$ , so that

$$X_{vn}^{(m)}(t) = f_v(\epsilon_n, \dots, \epsilon_{n-m+1}, \epsilon_{n-m}^*, \epsilon_{n-m-1}^*, \dots),$$

where  $\epsilon_n^*$  is an independent copy of  $\epsilon_n$ , and

$$\sum_{m=0}^{\infty} \{E\|X_{vn}(t) - X_{vn}^{(m)}(t)\|^{4+\delta}\}^{1/(4+\delta)} < \infty.$$

**Assumption 2.** For an arbitrary community  $\mathcal{K} \subseteq \{1, \dots, G\}$ , the eigenvalues of the operator  $\sum_{v \in \mathcal{K}} \Gamma_v(\cdot)$  are distinct.

**Assumption 3.** For each  $v$ , the covariance operator  $\Gamma_v(\cdot)$  admits the spectral decomposition  $\Gamma_v(\cdot) = \sum_{j \geq 1} \theta_{vj} \langle \phi_{vj}, \cdot \rangle \phi_{vj}$ , such that  $\sum_{j \geq 1} \theta_{vj}$  remains constant across  $v$ . In addition, for each  $v$ , there exists some  $p_v > 2$ , so that  $\theta_{vj} - \theta_{v,j+1} \geq \text{const.} j^{-p_v}$ .

**Assumption 4.** There exists  $c_0 > 0$ , so that  $\inf_{\alpha} |\beta_{1,\alpha} - \tau| > c_0$  and  $\inf_{\alpha} |\beta_{2,\alpha} - \tau| > c_0$ .

**Assumption 5.** Let  $M = G^{-1} \sum_{v=1}^G N_v$  and  $p = \max_v p_v$ , and assume that  $0 < \lim_{M \rightarrow \infty} N_{v_1}/N_{v_2} < \infty$  for arbitrary  $v_1, v_2 = 1, \dots, G$ , and  $D = M^{1/\gamma}$  where  $\gamma > 2(p + \tau + 1)$ .

**Assumption 6.** For arbitrary  $\tau_1 > \tau_2$  such that  $\mathcal{H}_{\tau_1} \neq \emptyset$  and  $\mathcal{H}_{\tau_2} \neq \emptyset$ ,  $\aleph \tilde{\mathbf{C}}_{\tau_1,1:D} > \aleph \tilde{\mathbf{C}}_{\tau_2,1:D}$  asymptotically almost surely as  $D \rightarrow \infty$ .

Assumption 1 indicates that the functions in all the groups are weakly dependent. Assumption 2 assures the identifiability of the filt-fPCs. Assumption 3 restricts that the total variation of different groups are on the same level, and sometimes a rescaling step becomes a necessity to make this assumption hold. Assumption 4 assures the identifiability of  $\mathcal{H}_{\tau}$ . Assumption 5 indicates that there are no trivial groups, and  $\gamma > 2(\kappa + \tau + 1)$  prevents the estimation error to be overly large. Assumption 6 indicates that a more accurate filt-fPC representation leads to more communities incorporated.

Define  $\Delta \aleph_{\alpha,d}^{\tau} = \aleph \mathbf{C}_{\alpha,1:d} - \aleph \tilde{\mathbf{C}}_{\tau,1:d}$ . With Assumptions (1)–(6), we now develop the theorem stated below, which illustrates the conditions under which a  $\tau$ -oracle community structure can be found with probability 1 asymptotically, and also essentially demonstrates how the selection of the tuning parameter  $\lambda_N$  influences the efficiency (ability of function reconstruction with respect to mean squared error of truncated filt-fPC representation) of the resulting filt-fPCs.

**Theorem 1.** Suppose that Assumptions (1)–(6) hold, and  $\mathcal{H}_{\tau} \neq \emptyset$ , if  $\lambda_N$  satisfies the following conditions

$$\begin{aligned} \max_{\alpha} \{M^{\beta_{1,\alpha}/\gamma} \Delta \aleph_{\alpha,D}^{\tau}\} \lambda_N &\rightarrow 0, & \mathbf{C}_{\alpha} \in \mathcal{H}_{\tau,-} \\ M^{\tau/\gamma} \min_{\alpha} \{\Delta \aleph_{\alpha,D}^{\tau}\} \lambda_N &\rightarrow \infty, & \mathbf{C}_{\alpha} \in \mathcal{H}_{\tau,+}, \end{aligned}$$

In addition, denote  $\tilde{\sigma}_{\tau,D}$  as the  $\sigma_{\alpha,D}$  under a  $\tau$ -oracle community structure, and assume that for  $\mathbf{C}_\alpha \in \mathcal{H}_\tau$

$$|\sigma_{\alpha,D} - \tilde{\sigma}_{\tau,D}| = o(\min_{\alpha} \{\Delta \aleph_{\alpha,D}^\tau\} \lambda_N), \quad M^{1/2-(p+1)/\gamma} \min_{\alpha} \{\Delta \aleph_{\alpha,D}^\tau\} \lambda_N \rightarrow \infty,$$

the selected community structure  $\hat{\mathbf{C}}$  by minimizing (3-2) is a  $\tau$ -oracle community structure asymptotically almost surely.

**Remark 8.** The cardinality difference  $\Delta \aleph_{\alpha,D}^\tau$  depends on the employed community detection algorithm, which is typically an unsupervised learning procedure.

Here we briefly explain the assumptions in the theorem. When  $\mathbf{C}_\alpha \in \mathcal{H}_{\tau,-}$ , it is not selected because the representation of the corresponding filt-fPCs is not as efficient as that of  $\tau$ -oracle community structure. Thus one would have to restrict that the superiority of representation accuracy of the filt-fPC obtained from  $\tilde{\mathbf{C}}_\tau$  to be more pronounced than the difference of cardinality. The reasoning is similar but is at the other end of the spectrum when  $\mathbf{C}_\alpha \in \mathcal{H}_{\tau,+}$ . When  $\mathbf{C}_\alpha \in \mathcal{H}_\tau$ , the difference of the representation accuracy is typically very small, and the  $\tau$ -oracle community structure is selected when the superiority of cardinality (more parsimonious) is pronounced, and it is necessary to require that the estimation error is not too large.

A drawback of the selection procedure based on the above GIC criterion is the high number of possible community structures if  $G$  is large, making it very computationally costly to obtain the GIC values for all structures. To overcome this limitation, we propose another iterative procedure described below.

### 3.4.2 Iterative selection of thresholds

In the algorithm, the selection of thresholds determines the community structure. We propose the following iterative GIC selection procedure. Denote the empirical filt-fPC score as  $Z_{vn,d} = \langle R_{vn}^{(d-1)}, \hat{\phi}_d^{(c_{v,d})} \rangle$ , then the GIC value at layer  $d$  is

$$\text{GIC}(\mathbf{C}_d) = - \sum_{v=1}^G f_v \left\{ N_v^{-1} \sum_{n=1}^{N_v} Z_{vn,d}^2 \right\} + \kappa_N(d) \aleph \mathbf{C}_d,$$

where  $\kappa_N(d)$  is a non-increasing function with respect to  $d$ , indicating more idiosyncratic features are to be obtained as  $d$  increases. We propose to select the threshold  $\tau_d$ , such that the resulting  $\hat{\mathbf{C}}_d$  and  $\{\hat{\phi}_d^{(c_{v,d})}(t) : v = 1, \dots, G\}$  minimize the above quantity. Suppose that the  $(d-1)$ -th threshold is  $\tau_{d-1}$ , then the  $d$ -th threshold is searched along the interval  $[0, \tau_{d-1}]$  (note that a common threshold can be employed for consecutive multiple, or even infinitely many, layers). In order to minimize computational burden, the thresholds are selected from finite number of threshold candidates, where each candidate truncates at least one more edge than the larger candidates.

It is noted that the number of tuning parameters  $\{\kappa_N(d) : d = 1, \dots, D\}$  increases as  $D$  diverges. To reduce the complexity of tuning parameter selection, our proposal is to

employ some parametric form for  $\kappa_N(d)$ , e.g.,  $\kappa_N(d) = ad^{-b}$  or  $\kappa_N(d) = ab^{-d}$ . A large-valued and slow-decaying sequence  $\{\kappa_N(d): d \geq 1\}$  typically leads to a parsimonious but inefficient filt-fPC representation. In principle, the dimension  $D$  is selected so that the first  $D$  filt-fPCs capture most variation (e.g., 80%) for each group. The values  $a, b$  should be selected so that the resulting filt-fPCs is parsimonious and efficient in functional reconstruction (e.g., the  $D$ -layers community structure explains 80% variance for each group with the minimal cardinality  $\aleph \mathbf{C}_{1:D}$ ). In other words, the selection of  $D$  and  $\{\kappa_N(d): d = 1, \dots, D\}$  is data driven that uses the scree plots and cardinality plot.

Denote the community structure selected by the iterative GIC procedure as  $\hat{\mathbf{C}}_{iter}$ . The following theorem demonstrates that, under some regularity conditions on  $\{\kappa_N(d): d \geq 1\}$ , the iteratively selected community structure will not fall into the under-fitted class if the sample size is large enough, which theoretically guarantees the good performance of the proposed iterative procedure.

**Theorem 2.** If Assumption (1)–(6) hold and  $\lambda_N = \sum_{d \geq 1} \kappa_N(d)$  satisfies the first condition in Theorem 1, say,  $\max_{\alpha} \{M^{\beta_{1,\alpha}/\gamma} \Delta \aleph_{\alpha,D}^{\tau}\} \lambda_N \rightarrow 0$ , for  $\mathbf{C}_{\alpha} \in \mathcal{H}_{\tau,-}$ . Additionally if  $M^{-1/2} \sum_{d=1}^D d^p \kappa_N^{-1}(d) \rightarrow 0$ , then  $\hat{\mathbf{C}}_{iter} \notin \mathcal{H}_{\tau,-}$  asymptotically almost surely.

**Remark 9.** This theorem gives a uniform condition under which the iterative GIC selection procedure is guaranteed to produce decent community structure for efficient filt-fPC approximation when the sample size is large enough, regardless of the structure of  $\hat{\mathbf{C}}_{iter}$ .

### 3.5 Centroid-based community detection

Community detection (CD), or graph partition, is a tool that is widely used to extract the hidden relation among the nodes in a network. A popular principle of the existing community detection algorithms for weighted network is making the nodes within a community more closely connected than nodes in different communities. The result of such algorithm is that the total within-community degree is significantly smaller (if small value of edge weight indicates stronger connection) than the total between-community degree (see e.g., Lu et al. (2013), Shen et al. (2016) and Palowitch et al. (2017)). However, the goal in this paper is to find the common principal components that jointly explain the variation of different groups with a parsimonious filt-fPC representation, and the aim of the conventional algorithms is obviously different from the goal of filt-fPCA, and thus may not lead to a parsimonious representation. This has been the motivation for developing a more suitable community detection algorithm.

The idea of our community detection algorithm comes from the fact that, given three covariance operators  $\Gamma_1, \Gamma_2, \Gamma_3$ , if  $\|\Gamma_1 - \Gamma_2\|_{\mathcal{S}}$  and  $\|\Gamma_2 - \Gamma_3\|_{\mathcal{S}}$  are small, then  $\|\Gamma_1 - \Gamma_3\|_{\mathcal{S}}$  should also be small by the triangle inequality of the Hilbert-Schmidt norm (the standard for "small" varies according to the non-ascending thresholds). Define the centroid node  $v_c$  of the community  $\mathcal{K}$  to be the node with the smallest within-community

degree (node degree is defined as the summation of weight of edges adjacent to the node); and the community  $\mathcal{K}_{v_c}$  as the collection of nodes that are connected to the centroid node  $v_c$  (including  $v_c$ ). We iterate between detecting the centroid node, and expanding the community by finding all the nodes connected to the centroid node till the community results become stable. A detailed pseudocode can be found in the supplementary material.

**Remark 10.** The community detection algorithm that can be applied here is not unique. However, since developing community detection is not the focus of this paper, we do not introduce other applicable approaches here.

**Remark 11.** A large weight (e.g.,  $G \times \max_{i,j} \omega_{ij}$ ) can be set to the edges connecting different communities before searching the communities in the next layer, so that the selected communities are nested in those of the previous layers.

## 4 Simulation studies

The goal here is to investigate the ability of the filt-fPCs to capture the underlying structure of multi-group functions. In the simulations, samples were generated from the following model  $X_{vn}(t) = \sum_{d=1}^5 \xi_{vn,d} \psi_{vd}(t)$ , where  $\psi_{vd}(t)$  are orthonormal basis across both  $v$  and  $d$ . 500 functions were simulated for each of the 16 groups  $(\Pi_1, \dots, \Pi_{16})$ . To obtain  $\{\psi_{vd}(t) : v \geq 1, d \geq 1\}$ , 22 functions were first randomly simulated with 23 Fourier basis functions  $\{F_i(t) : i = 1, \dots, 23\}$ ,

$$F_i(t) = \begin{cases} 1, & \text{if } i = 1, \\ \sqrt{2} \cos(2\pi kt), & \text{if } i = 2k, \\ \sqrt{2} \sin(2\pi kt), & \text{if } i = 2k + 1. \end{cases}$$

The Gram-Schmidt process was applied to obtain 22 orthonormal basis functions

$$\{B_1(t), \dots, B_{22}(t)\}.$$

The scores  $\{\xi_{vn,d} : d = 1, \dots, 5\}$  are independent and follow normal distribution  $\mathcal{N}(0, 1.2^{-d})$  for  $v = 1, \dots, 12$ , and  $\mathcal{N}(0, 1.2^{d-6})$ , for group  $v = 13, \dots, 16$ . The five basis functions employed to generate functions in each group are shown in Table 1. The first 3 curves of each group are displayed in Figure 4.

The iterative GIC criterion was employed to detect the community structure, and the penalty term follows the form  $\kappa(d) = ad^{-b}$ . The selected candidates for  $a$  are 0.05, 0.1, 0.2, 0.3, 0.5, and for  $b$  are 1, 1.1, 1.2, 1.3, 1.4. Here we used the ratio

$$R = \sum_{v=1}^{16} \sum_{n=1}^{500} \|R_{vn}^{(5)}\|^2 \bigg/ \sum_{v=1}^{16} \sum_{n=1}^{500} \|X_{vn}\|^2$$

to evaluate the reconstruction performance of the estimated filt-fPCs. The corresponding ratio  $R$  according to different pairs of  $a, b$  are displayed in Table 2. A reasonable selection of  $a, b$  is 0.1, 1.3, and the corresponding community structure is

$$\text{1st layer : } (\Pi_1 - \Pi_{16}).$$

$v$	$\{\phi_{vd}(t) : d = 1, 2, 3, 4, 5\}$	$v$	$\{\phi_{vd}(t) : d = 1, 2, 3, 4, 5\}$
1	$B_1(t)B_2(t)B_3(t)B_4(t)B_5(t)$	9	$B_1(t)B_2(t)B_3(t)B_4(t)B_5(t)$
2	$B_1(t)B_2(t)B_3(t)B_4(t)B_6(t)$	10	$B_1(t)B_2(t)B_3(t)B_4(t)B_6(t)$
3	$B_1(t)B_2(t)B_7(t)B_8(t)B_9(t)$	11	$B_1(t)B_2(t)B_7(t)B_8(t)B_9(t)$
4	$B_1(t)B_2(t)B_7(t)B_8(t)B_{10}(t)$	12	$B_1(t)B_2(t)B_7(t)B_8(t)B_{10}(t)$
5	$B_1(t)B_{11}(t)\mathcal{B}_{12}(t)\mathcal{B}_{13}(t)\mathcal{B}_{14}(t)$	13	$B_1(t)B_{11}(t)\mathcal{B}_{12}(t)\mathcal{B}_{13}(t)\mathcal{B}_{14}(t)$
6	$B_1(t)B_{11}(t)\mathcal{B}_{12}(t)\mathcal{B}_{15}(t)\mathcal{B}_{16}(t)$	14	$B_1(t)B_{11}(t)\mathcal{B}_{12}(t)\mathcal{B}_{15}(t)\mathcal{B}_{16}(t)$
7	$B_1(t)B_{11}(t)\mathcal{B}_{17}(t)\mathcal{B}_{18}(t)\mathcal{B}_{19}(t)$	15	$B_1(t)B_{11}(t)\mathcal{B}_{17}(t)\mathcal{B}_{18}(t)\mathcal{B}_{19}(t)$
8	$B_1(t)B_{11}(t)\mathcal{B}_{20}(t)\mathcal{B}_{21}(t)\mathcal{B}_{22}(t)$	16	$B_1(t)B_{11}(t)\mathcal{B}_{20}(t)\mathcal{B}_{21}(t)\mathcal{B}_{22}(t)$

Table 1: Basis functions of different groups. The two halves are identical, but group 13–16 do not have the same covariance functions of group 5–8 as the scores follow different distributions.

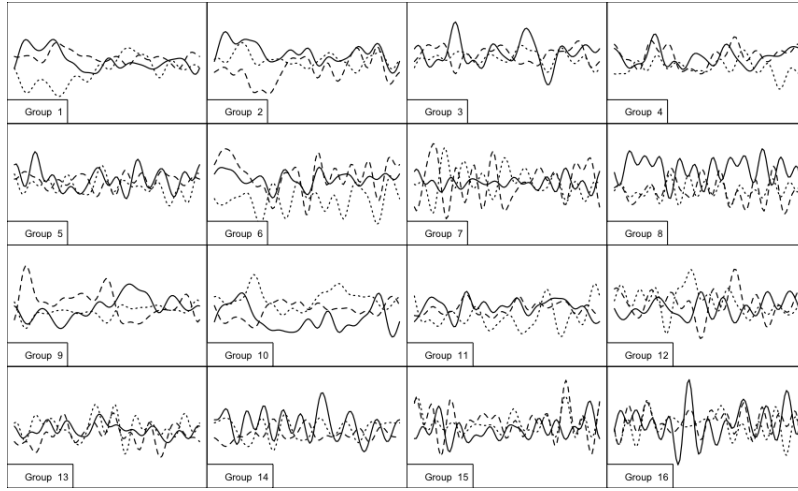


Figure 4: The first 3 simulated curves of each group

2nd layer :  $(\Pi_1 - \Pi_4, \Pi_9 - \Pi_{12}); (\Pi_5 - \Pi_8, \Pi_{13} - \Pi_{16});$   
3rd layer :  $(\Pi_1, \Pi_2, \Pi_9, \Pi_{10}); (\Pi_3, \Pi_4, \Pi_{11}, \Pi_{12});$   
 $(\Pi_5, \Pi_{13}); (\Pi_6, \Pi_{14}); (\Pi_7, \Pi_{15}); (\Pi_8, \Pi_{16}).$   
4th layer :  $(\Pi_1, \Pi_2, \Pi_9, \Pi_{10}); (\Pi_3, \Pi_4, \Pi_{11}, \Pi_{12});$   
 $(\Pi_5, \Pi_{13}); (\Pi_6, \Pi_{14}); (\Pi_7, \Pi_{15}); (\Pi_8, \Pi_{16}).$   
5th layer :  $(\Pi_1, \Pi_9); (\Pi_2, \Pi_{10}); (\Pi_3, \Pi_{11}); (\Pi_4, \Pi_{12});$   
 $(\Pi_5); (\Pi_6); (\Pi_7); (\Pi_8); (\Pi_{13}); (\Pi_{14}); (\Pi_{15}); (\Pi_{16}).$

Based on the result, both common and individual patterns of different groups are well preserved by the proposed filt-fPCs. Meanwhile, we can capture most information of the 16 groups with 27 distinct filt-fPCs instead of 80 ( $16 \times 5$ ) group-wise functional principal components. The hidden intrinsic structure is well captured by the filt-fPCs. In addition, the result is robust to the selection of the tuning parameters  $a, b$ .

**Remark 12.** Unlike ordinary fPCs, the order of the filt-fPCs of one individual group

$a \backslash b$	1	1.1	1.2	1.3	1.4
0.05	0.022 (38)	0.022 (38)	0.020 (42)	0.020 (42)	0.020 (42)
0.1	2.064 (21)	0.022 (27)	0.022 (27)	0.022 (27)	0.022 (35)
0.2	2.064 (21)	2.064 (21)	2.064 (21)	2.064 (21)	0.022 (27)
0.3	2.064 (21)	2.064 (21)	2.064 (21)	2.064 (21)	2.064 (21)
0.5	18.265 (9)	5.868 (17)	5.868 (17)	5.868 (17)	2.064 (21)

Table 2:  $R$  values (%) according to each pair of  $a, b$ , the value in the parenthesis is the total number of distinct filt-fPCs.

does not necessarily pertain to the importance of the filt-fPCs (proportion of variance explained) for the group. For example, in the simulation, the first common filt-fPC is the most important one for group 1–12, but not for group 13–16. However, since the first common filt-fPC also explains a sufficient large proportion of variance for group 13–16, it is detected and employed across all groups.

**Remark 13.** In simulation, the functions were generated by a pre-specified model. However, in practice, such "ground-truth" generative models are always unknown and hard to detect. One advantage of the filtration technique is that it always efficiently extracts informative fPC structure from any complex multi-group function data.

## 5 The analysis of rat brain local field potentials

Synchrony widely exists in brain signals, and is an important measure of temporal coordination between neuronal activities across the brain. A sudden increased scale of synchrony can indicate a rapidly emerging response from an extreme shock such as stroke. Here, we applied the proposed filt-fPCA to identify and quantify (by checking the variability explained by the common filt-fPCs) the changes in the synchrony structure of LFPs collected from a rat brain across 32 recorded regions.

### 5.1 Data processing and visualization

According to Wann (2017), increased large-scale spatiotemporal synchrony shortly after the occlusion onset (simulated ischemic stroke) is driven by low-frequency oscillations. Thus, the LFPs were bandpass filtered at  $(0, 10]$  Hertz and segmented into 1-second epochs for the pre-occlusion and post-occlusion phases separately. The same procedure



can also be employed for other frequency bands but we did not pursue it here. In the situation where structural breaks in the covariance structure are also of major concern, the first step is to detect these breakpoints (e.g., Jiao et al. (2022)), and then apply the proposed filt-fPCA method to each local quasi-stationary sub-sequence segmented by the detected break points. Here we considered the overall difference of variation pattern and hidden community structure between the pre-occlusion and post-occlusion epochs, so we conducted a global analysis for both phases.

Visualization reveals the occasional occurrence of irregular extreme values. Therefore, to stabilize the variance, we applied the square root transformation to the values of trajectories, specifically,  $\text{sign}(X_{vn}(t))\sqrt{|X_{vn}(t)|}$ . In addition, outlier epochs were removed from each tetrode under both phases, where outlier epochs *in each group* are defined as those of which the  $l^2$ -norm is beyond the interval  $[Q_1 - 1.5 \times \text{IQR}, Q_3 + 1.5 \times \text{IQR}]$ . Here  $\text{IQR} = Q_3 - Q_1$  and  $Q_1, Q_3$  are the first and third quantile of the  $l_2$ -norm of the epoch trajectories. Denote the covariance operator of the trajectories from the  $v$ -th tetrode to be  $\Gamma_{kv}$ ,  $k = 1, 2$ ,  $v = 1, \dots, 32$ , and all covariance operators were scaled by the summation of their eigenvalues, say,  $\mathcal{C}_{kv} = \Gamma_{kv} / \sum_{i \geq 1} \theta_{kv,i}$ . Here,  $k = 1$  indicates the pre-occlusion phase and  $k = 2$  refers to the post-occlusion phase.

Two networks  $(N, E, \omega_1)$ ,  $(N, E, \omega_2)$  were constructed for the pre-occlusion and post-occlusion epochs separately. The node set  $N$  has 32 nodes representing the 32 tetrodes, and the edge set  $E$  is complete which means all nodes are connected initially. Figure 5 displays the Hilbert Schmidt norm  $\omega_{k,ij} = \|\mathcal{C}_{ki} - \mathcal{C}_{kj}\|_{\mathcal{S}}$ ,  $k = 1, 2$ ,  $i, j = 1, \dots, 32$ , which serve as the edge weights in the analysis.

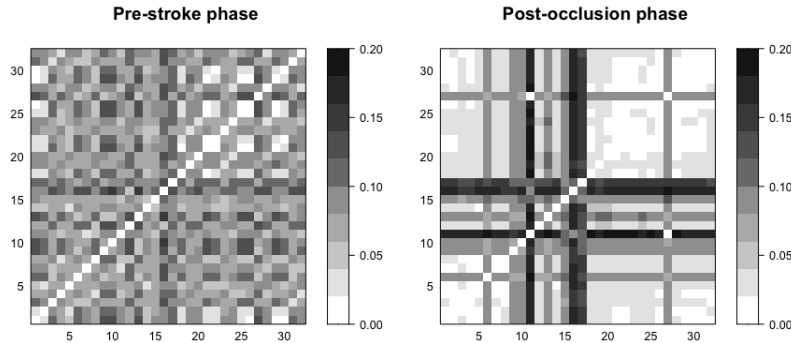


Figure 5:  $\|\mathcal{C}_{ki} - \mathcal{C}_{kj}\|_{\mathcal{S}}$ ,  $i, j = 1, \dots, 32$ ,  $k = 1, 2$ .

From Figure 5, we see that after the occlusion onset, the epoch trajectories from most of the 32 tetrodes display more similar variation patterns due to the increased larger-scale signal-synchrony. Therefore, a more parsimonious filt-fPC representation is expected for the post-occlusion phase. The weight matrix changes substantially after the occlusion onset, making it necessary to implement filt-fPCA to the two phases separately. Figure 6 shows the average weights of edges adjacent to each node, defined as  $\sum_{j=1}^{32} \omega_{k,ij} / 32$ ,  $i = 1, 2, \dots, 32$ . Clearly, a large portion of weights shrink after the occlusion onset due to the increased signal-synchrony.

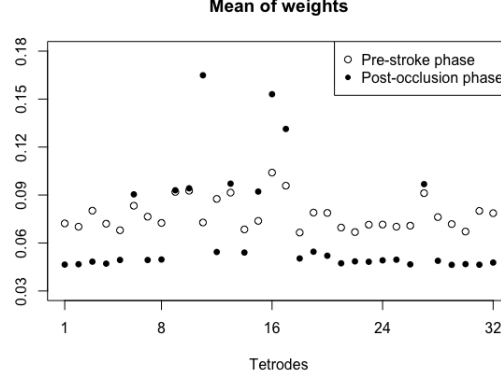


Figure 6: Average weights of edges adjacent to each node

## 5.2 Permutation test on the discrepancy of edge weights

We employed the permutation method to test the significance of the discrepancy between weight matrices  $\omega_1, \omega_2$ . After the pre-processing, the resulting epochs of different tetrotodes were permuted simultaneously to form new sequences of epochs  $\{X_{vn}^{(b)} : v = 1, \dots, 32, n = 1, \dots, N_v\}$ . This permutation of the combined set of pre-occlusion and post-occlusion epochs is justified under the null hypothesis. The sequence of the permuted trajectories were segmented at the occlusion time, and for each  $v$ , the first segment ( $I_{1v}$ ) trajectories were used to calculate the covariance operator  $\hat{\Gamma}_{1v}^{(b)}$ , while the second segment ( $I_{2v}$ ) trajectories were used to obtain the covariance operator  $\hat{\Gamma}_{2v}^{(b)}$ , defined as

$$\hat{\Gamma}_{1v}^{(b)}(\cdot) = (\#I_{1v})^{-1} \sum_{n \in I_{1v}} X_{vn}^{(b)} \langle X_{vn}^{(b)}, \cdot \rangle, \quad \hat{\Gamma}_{2v}^{(b)}(\cdot) = (\#I_{2v})^{-1} \sum_{n \in I_{2v}} X_{vn}^{(b)} \langle X_{vn}^{(b)}, \cdot \rangle,$$

where  $\#$  signifies the sample size. The covariance operators were scaled by the summation of their eigenvalues to obtain  $\hat{\mathcal{C}}_{1v}^{(b)}$  and  $\hat{\mathcal{C}}_{2v}^{(b)}$ , then obtained the Hilbert-Schmidt norm  $\|\hat{\mathcal{C}}_{ki}^{(b)} - \hat{\mathcal{C}}_{kj}^{(b)}\|_S$ , denoted as  $\omega_{k,ij}^{(b)}$ ,  $k = 1, 2$ . The discrepancy were evaluated by the Frobenius norm  $D_b = \|\omega_1^{(b)} - \omega_2^{(b)}\|_F$ . The procedure was repeated for  $B = 10,000$  times, and the Frobenius norm  $\|\omega_1 - \omega_2\|_F$  was found greater than the 99% quantile of  $D_1, \dots, D_B$ . Thus the discrepancy of weight matrices is significant, making the comparison reasonable and necessary.

## 5.3 Community detection and filt-fPCs

The proposed iterative GIC selection procedure was employed to select the community structure. To conduct a fair comparison for the community structures between the two brain phases, we set  $\kappa(d) = 0.01 \times d^{-1.4}$ , which produces decent filt-fPC representation for both phases. Here, it is assumed that all groups are equally important, and for any  $d$ , set  $f_v^{(d)} = 1 / \sum_{j \geq 1} \theta_{vj}^{(d-1)}$  for  $v = 1, \dots, 32$ . The first four layers' filt-fPCs of pre-occlusion and post-occlusion trajectories are presented in the supplementary material.

To demonstrate the efficiency of the filt-fPC representation, we calculated the approximation error of the first  $D$  ( $D = 1, \dots, 20$ ) empirical filt-fPCs for each tetrode  $v$ , defined as

$$e_{vD} = \frac{1}{N_v} \sum_{n=1}^{N_v} \left\| X_{vn}(t) - \sum_{d=1}^D \langle X_{vn}, \hat{\phi}_d^{(c_{v,d})} \rangle \hat{\phi}_d^{(c_{v,d})}(t) \right\|.$$

For comparison, the above errors were also computed for ordinary group-wise fPCs. Figure 1 and Figure 2 in the supplementary material present the approximation errors of trajectories from the 32 tetrodes with 1 – 20 filt-fPCs and group-wise ordinary fPCs, and clearly, the reconstruction performance of the empirical filt-fPCs are similar to that of group-wise ordinary fPCs.

Figure 7 and 8 show the community detection results (first 8 layers, see the supplementary material for the whole 20 layers) under the two phases, where the points (representing tetrodes, displayed in the same order as in the experiment) with the same color and shape are in the same community. Clearly, after the occlusion onset, most tetrodes were clustered in the same community, leading to a much more parsimonious filt-fPC representation. The total number of distinct communities drops from 223 to 94 after the occlusion onset. Scaled chord diagrams (Figure 9) of the number of shared filt-fPCs are displayed to show the sub-structure of synchrony. Combining Figure 1, 2 in the supplementary material, it is clear that tetrode 11, 16, 17 form a sub-structure with shared filt-fPC explaining 40%–50% of the total variability for each of these three group after the occlusion onset, while only 20%–30% before the occlusion onset. In addition, the sub-structure of synchrony formed by tetrode 6, 9, 10, 13, 27 consistently exists regardless of the phase and the shared filt-fPCs explain 50%–60% of the total variability for each of these tetrode before the occlusion onset, and 100% after the occlusion onset. After the occlusion onset, the rest tetrodes are highly synchronized and share the same set of filt-fPCs. This suggests a new and interesting finding which is, immediately following a shock to the system, the neuronal activity at the tetrodes are highly synchronized. One interpretation here is that an extreme event such as the sudden lack of oxygen delivered caused the neurons to respond in a similar manner. It is interesting that this phenomenon is also observed in financial data, i.e., a severe drop in the market elicits similar and synchronized behavior in stocks.

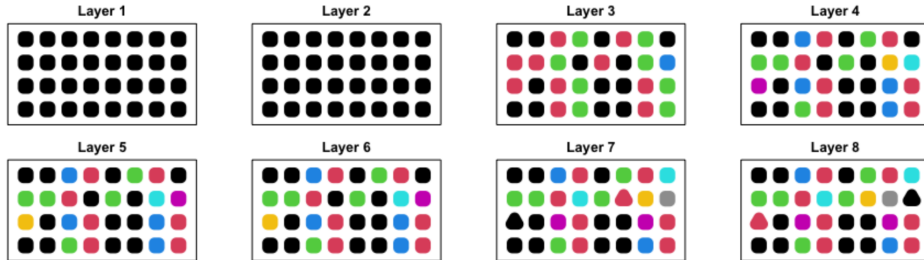


Figure 7: Community structures of pre-occlusion phase

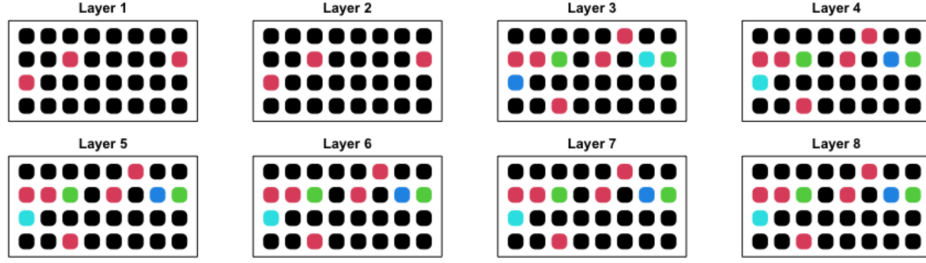


Figure 8: Community structures of post-occlusion phase

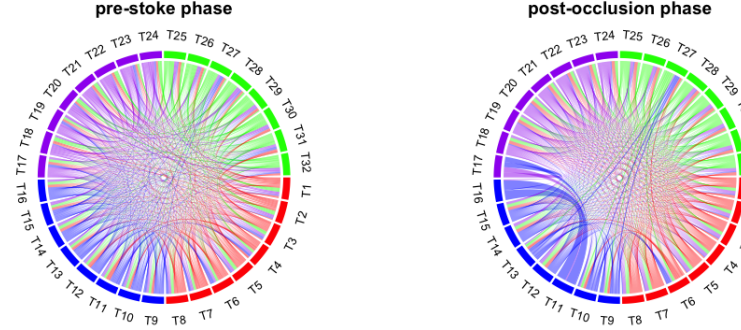


Figure 9: Scaled chord diagram of the number of shared layers (20-layers filtration). Tetraode 11, 16 and 17 display substantially different variation pattern after the occlusion onset. The synchrony of the tetraode 6, 9, 10, 13, 27 is strengthened after the occlusion onset.

## 5.4 Summary of the analysis of the rat stroke LFP data

Large-scale synchrony occurred due to the ischemic stroke. After the occlusion onset, the epoch trajectories collected from tetraode 11, 16, 17 present much more different covariance structure comparing with the trajectories collected from other tetrodes, while substantial common variation patterns are also significantly present among them, making these tetrodes separated from the others in the first layer. The synchrony structure of tetraode 6, 9, 10, 13, 27 consistently existed regardless of the brain phase, and was substantially enhanced by the occlusion. For the rest tetrodes, occlusion substantially enhanced the synchrony so that common components are able to capture most of the epoch variability after the occlusion onset. Overall speaking, the sudden lack of oxygen caused by artery stroke made most of the brain behave more similarly.

## 6 Conclusions

Local field potentials provide information about brain function. They are collected from multiple tetrodes inserted on a pre-arranged patch on the cortex. The trajec-

ries collected from different tetrodes simultaneously can be considered as multi-group functional data. Synchrony of different tetrodes potentially indicates functional connectivity of different regions of brain and a suddenly increased scale of spontaneous neuronal synchrony may antecede neuronal activity impairments in ischemic studies. The filt-fPC analysis provides a novel and efficient way to extract and quantify the multi-layer synchrony structure of multi-tetrode LFP recordings by employing filtrated common functional principal components. We developed a data-driven algorithm to find the filtrated common functional principal components. Specifically, we first specify a tree-structured community structure for the weighted network, established from data to measure the similarity of covariance structures of different tetrodes of epochs, and then find the common filt-fPCs for every community. The application of filt-fPCA to the local field potentials not only reveal the large-scale synchrony phenomenon after the occlusion onset, but also quantify the changes of synchrony. The method is developed *not* only for the LFP data described in this paper, but for all kinds of multi-group functional data, such as longitudinal functional data, multivariate functional data and spatial-temporal data.

The filt-fPCA have several advantages: (1.) The method is data driven, can be implemented without prior-knowledge, and is not constrained by model pre-specification, making it suitable for any complex case. (2.) The method is able to extract the common variation patterns of different groups of functions in a novel "multi-resolution" manner, and the obtained filt-fPCs are efficient in functional reconstruction. (3.) The method can be applied to both balanced and unbalanced design. (4.) The filtrated functional principal components are orthogonal to each other for each group, leading to a concise basis representation. Extending filtration techniques to functional linear models will be pursued as future work.

## References

- Bali, J. L., Boente, G., Tyler, D. E. & Wang, J.-L. (2011), ‘Robust functional principal components: A projection-pursuit approach’, *The Annals of Statistics* **39**(6), 2852–2882.
- Benko, M., Härdle, W. & Kneip, A. (2009), ‘Common functional principal components’, *The Annals of Statistics* **37**(1), 1–34.
- Berrendero, J. R., Justel, A. & Svarc, M. (2011), ‘Principal components for multivariate functional data’, *Computational Statistics & Data Analysis* **55**(9), 2619–2634.
- Chen, K., Delicado Useros, P. F. & Müller, H.-G. (2017), ‘Modelling function-valued stochastic processes, with applications to fertility dynamics’, *Journal of the Royal Statistical Society. Series B, Statistical Methodology* **79**(1), 177–196.
- Chen, K. & Müller, H.-G. (2012), ‘Modeling repeated functional observations’, *Journal of the American Statistical Association* **107**(500), 1599–1609.

- Chiou, J.-M., Chen, Y.-T. & Yang, Y.-F. (2014), ‘Multivariate functional principal component analysis: A normalization approach’, *Statistica Sinica* pp. 1571–1596.
- Crainiceanu, C. M., Caffo, B. S., Luo, S., Zipunnikov, V. M. & Punjabi, N. M. (2011), ‘Population value decomposition, a framework for the analysis of image populations’, *Journal of the American Statistical Association* **106**(495), 775–790.
- Di, C., Crainiceanu, C. M. & Jank, W. S. (2014), ‘Multilevel sparse functional principal component analysis’, *Stat* **3**(1), 126–143.
- Di, C.-Z., Crainiceanu, C. M., Caffo, B. S. & Punjabi, N. M. (2009), ‘Multilevel functional principal component analysis’, *The annals of applied statistics* **3**(1), 458.
- Feng, Q., Jiang, M., Hannig, J. & Marron, J. (2018), ‘Angle-based joint and individual variation explained’, *Journal of multivariate analysis* **166**, 241–265.
- Flury, B. K. (1987), ‘Two generalizations of the common principal component model’, *Biometrika* **74**(1), 59–69.
- Flury, B. N. (1984), ‘Common principal components in k groups’, *Journal of the American Statistical Association* **79**(388), 892–898.
- Greven, S., Crainiceanu, C., Caffo, B. & Reich, D. (2011), Longitudinal functional principal component analysis, in ‘Recent Advances in Functional Data Analysis and Related Topics’, Springer, pp. 149–154.
- Hall, P. & Hosseini-Nasab, M. (2006), ‘On properties of functional principal components analysis’, *Journal of the Royal Statistical Society: Series B (Statistical Methodology)* **68**(1), 109–126.
- Hall, P., Müller, H.-G. & Wang, J.-L. (2006), ‘Properties of principal component methods for functional and longitudinal data analysis’, *The annals of statistics* pp. 1493–1517.
- Happ, C. & Greven, S. (2018), ‘Multivariate functional principal component analysis for data observed on different (dimensional) domains’, *Journal of the American Statistical Association* **113**(522), 649–659.
- Hörmann, S. & Kokoszka, P. (2010), ‘Weakly dependent functional data’, *The Annals of Statistics* **38**(3), 1845–1884.
- Jacques, J. & Preda, C. (2014), ‘Model-based clustering for multivariate functional data’, *Computational Statistics & Data Analysis* **71**, 92–106.
- Jiang, C.-R. & Wang, J.-L. (2010), ‘Covariate adjusted functional principal components analysis for longitudinal data’, *The Annals of Statistics* **38**(2), 1194 – 1226.
- Jiao, S., Frostig, R. & Ombao, H. (2022), ‘Break point detection for functional covariance’, *arXiv:2006.13887*.

- Kayano, M. & Konishi, S. (2009), ‘Functional principal component analysis via regularized gaussian basis expansions and its application to unbalanced data’, *Journal of Statistical Planning and Inference* **139**(7), 2388–2398.
- Lock, E. F., Hoadley, K. A., Marron, J. S. & Nobel, A. B. (2013), ‘Joint and individual variation explained (jive) for integrated analysis of multiple data types’, *The annals of applied statistics* **7**(1), 523.
- Lu, Z., Wen, Y. & Cao, G. (2013), Community detection in weighted networks: Algorithms and applications, in ‘2013 IEEE International Conference on Pervasive Computing and Communications (PerCom)’, IEEE, pp. 179–184.
- Nishii, R. (1984), ‘Asymptotic properties of criteria for selection of variables in multiple regression’, *The Annals of Statistics* pp. 758–765.
- Palowitch, J., Bhamidi, S. & Nobel, A. B. (2017), ‘Significance-based community detection in weighted networks’, *The Journal of Machine Learning Research* **18**(1), 6899–6946.
- Ramsay, J. O. & Silverman, B. W. (2004), ‘Functional data analysis’, *Encyclopedia of Statistical Sciences* **4**.
- Schott, J. R. (1999), ‘Partial common principal component subspaces’, *Biometrika* **86**(4), 899–908.
- Shen, Y., Liu, Y. & Xing, W. (2016), ‘Community detection in weighted networks via recursive edge-filtration’, *Journal of Communications* **11**(5), 484–490.
- Wang, B., Luo, X., Zhao, Y. & Caffo, B. (2019), ‘Semiparametric partial common principal component analysis for covariance matrices’, *bioRxiv* p. 808527.
- Wann, E. G. (2017), Large-scale spatiotemporal neuronal activity dynamics predict cortical viability in a rodent model of ischemic stroke, PhD thesis, UC Irvine.
- Yao, F. (2007), ‘Functional principal component analysis for longitudinal and survival data’, *Statistica Sinica* pp. 965–983.
- Yao, F. & Lee, T. C. (2006), ‘Penalized spline models for functional principal component analysis’, *Journal of the Royal Statistical Society: Series B (Statistical Methodology)* **68**(1), 3–25.
- Zhang, Y., Li, R. & Tsai, C.-L. (2010), ‘Regularization parameter selections via generalized information criterion’, *Journal of the American Statistical Association* **105**(489), 312–323.